RSC Advances

ROYAL SOCIETY OF CHEMISTRY

www.rsc.org/advances

Journal Name

ARTICLE

Electrical characteristics of InGaZnO thin film transistor by co-sputtering dual InGaZnO and ZnO targets

Received 00th January 20xx,
Accepted 00th January 20xx

DOI: 10.1039/x0xx00000x

www.rsc.org/

Nidhi Tiwari,*[a] Ram Narayan Chauhan,[b] Po-Tsun Liu [a] and Han-Ping D. Shieh [a]

A co-sputtering of dual InGaZnO and ZnO targets, abbreviated by ZnO co-sputtered IGZO, is used to fabricate a high performance indium gallium zinc oxide (IGZO) thin film transistor in this work. The ZnO co-sputtered IGZO thin film exhibits smooth (R_{rms} ~ 0.29 nm), featureless, and amorphous structure with high carrier density (n ~ 4.29 × 10^{17} cm^{-3}). The performance and stability of ZnO co-sputtered IGZO TFT has been investigated and compared with the counterparts fabricated by a single ZnO and a-IGZO target respectively. Highest linear field effect mobility of 16.1 cm^2/Vs with an I_{on}/I_{off} ratio of 1.04 × 10^7, saturation drain current of 3.8 μA at 5V, and the lowest threshold voltage of 2.0 V with sub-threshold swing of 0.21V/dec have been obtained for the ZnO co-sputtered IGZO TFT. Furthermore, the ZnO co-sputtered IGZO TFT exhibited only a threshold voltage shift (ΔV_{th}) of 2.75 V under negative biased illuminated stress conditions for 2500s, whereas the IGZO and ZnO based TFTs suffered from a huge threshold voltage shift (ΔV_{th} > 6 V) under the same conditions. The obtained performance and stability of TFTs with ZnO co-sputtered IGZO film is very promising for low voltage displays applications.

1. Introduction

Zinc oxide based thin film transistors (TFT) viz., indium zinc oxide (IZO), zinc tin oxide (ZTO), and indium gallium zinc oxide (IGZO) have been actively investigated as replacement for silicon based TFTs in the backplanes of next-generation liquid crystal (LC) and active matrix organic light-emitting diode (AMOLED) displays.[1] The TFTs in the displays need low temperature deposition of semiconductors with high performance and high optical transparency. The materials integration and device structure design play a crucial role for optimizing the TFTs performance.[2,3] For example, a highly doped buried layer of gallium-zinc-oxide (GZO thickness ~ 25 nm) in a-IGZO channel layer (thickness ~ 25 nm) has been deposited at 200°C in Ar ambient for resulting TFT with field effect mobility (μ_{FE} ~ 10.04 cm^2/Vs), subthreshold swing (SS ~ 0.93V/decade), threshold voltage (V_{th} ~ 1.2V), and exhibited good stability (ΔV_{th} = 0.94V).[4] Liu et. al., prepared amorphous nitrogenated IGZO thin film (thickness ~ 50 nm) by d.c. sputtering at power of 100 W in Ar (flow rate ~ 10 sccm) ambient on the a-IGZO active channel layer (thickness ~ 50 nm) to protect the a-IGZO layer from UV light for enhancing the bilayer TFT reliability and stability.[5] In turn, bilayer ZnO (60 nm)/IGZO (50 nm) thin film has recently been deposited at 450°C in Ar: O_2 ambient for resulting a better TFT with μ_{FE} ~ 2.2 cm^2/Vs, SS ~ 0.52V/decade, V_{th} ~ 1.3V.[6] Double-stacked hafnium doped indium zinc oxide (HIZO thickness ~ 50 nm) was realized on gate insulator of SiN_x(400 nm)/SiO_x(50 nm) through r.f. sputtering at room temperature in Ar/O_2 (1:10) ambient at chamber pressure of 3mtorr and the r.f. power of 80 W to propose a-HIZO TFT with staggered bottom gate structure. The resulting TFT showed high field effect mobility ~ 15 cm^2/Vs with better stability (ΔV_{th} ~ -2.55V) under bias illumination.[7] Kim et. al., cosputtered copper (Cu) and gallium-indium-zinc oxide (GIZO) target to make a thin layer of Cu-In-Ga-Zn-O (CIGZO) on an a-GIZO active layer (thickness ~ 70 nm) for demonstrating a highly reliable stable TFT. The TFT showed the reliable performance (μ_{FE} ~ 5.1cm^2/Vs, SS ~ 0.68V/decade, V_{th} ~ 3.25V) with excellent stability (ΔV_{th} < 0.6V) at 3μA drain current under 60°C for 100h.[8] Recently, Li doped ZnO and spray coated ZnO thin films have been deposited at temperature ~ 300-400°C for utilizing as active channel layer in TFTs with improved device performance (mobility ~7.3-10 cm^2/Vs, V_{th}~-23.8V, SS ~0.44V/dec).[9,10] However, there is still a challenge for finding a way to attain improved stability while maintaining high-performances via novel oxide materials and post-treatment.[11,12]

In this work, three types of oxide thin films as the channel layer for TFT device are proposed to study their structural, roughness, electrical and chemical analysis for flat panel

[a, a*] Department of Photonics and Display Institute, National Chiao Tung University, Hsinchu, Taiwan, R.O.C., 30010, Fax: +886-3-5737681; Tel: +886-978-628-446; E-mail: nidhi1611@gmail.com, ptliu@mail.nctu.edu.tw,hpshieh@mail.nctu.edu.tw
[b] Department of Mechanical Engineering, Vignan University, Guntur-Andhra Pradesh- 522213, India, Tel: +91-8008357245; E-mail: chauhanramnarayan@gmail.com

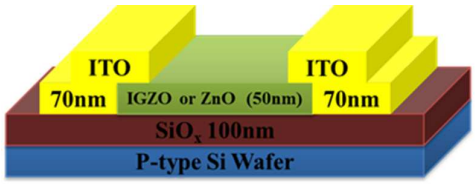

Fig. 1 Schematic diagram of TFT device.

displays (FPDs) applications. The first one is ZnO thin film and the second is IGZO film prepared by single target of InGaZnOx, as well as the IGZO deposited by dual targets of IGZO and ZnO referred as ZnO co-sputtered IGZO. In addition, the impact of film characteristics on the performance and stability of ZnO co-sputtered IGZO TFT has been investigated and compared with the conventional a-IGZO and ZnO based TFTs.

2. Experimental

The ZnO, IGZO and ZnO co-sputtered IGZO thin films (thickness ~50 nm) were deposited on SiO_2/Si and glass substrates at room temperature by dual RF magnetron sputtering with IGZO and ZnO targets of 99.99% purity. The system was evacuated to 2×10^{-6} mbar prior to introducing Ar:O_2 (10:0.6) gas at a chamber pressure of 3 mtorr for sputtering of ZnO and IGZO target at a rate of 0.26 and 0.3 $Å s^{-1}$, respectively, by RF magnetron sputtering at the same power of 80 W. The films were annealed at 425°C for 1h in N_2 environment. The structure, morphology, roughness, chemical, and electrical properties of the films on glass substrates were investigated by using X-ray diffraction (XRD, Bede-D[1]), Transmission electron microscope (TEM, JEOL-JEM-2100F), Nanoscope SPM V5, PHI 5000 versa probe II by using monochromatic Al Kα radiation (1486.6 eV) and Hall measurement, respectively.

The ZnO co-sputtered IGZO thin film (thickness ~ 50 nm) was utilized as an active channel layer, SiO_2 (thickness ~100 nm) as an insulator and Si as a gate for TFT fabrication. The drain and source (thickness ~70 nm) were sputter deposited at a rate of $0.27 Å s^{-1}$ on the active channel layer through shadow mask by using In_2O_3:SnO_2 (90:10wt. %) target of 99.99% purity. During sputtering, the RF power and argon gas pressure in the chamber were maintained at 50 W, 3 mtorr, respectively. For sake of comparison, pure ZnO and a-IGZO based TFTs were also fabricated with the same configuration (Fig. 1). Further, the devices were annealed at 425°C for 1h in N_2 environment. The measured devices have an electrode width (W) of 1000 µm and a channel length (L) of 200 µm. All electrical characterizations were performed using a semi-conductor parameter analyzer (Keithley 4500C) in the dark at room temperature.

3. Results and discussion

3.1. Structure and morphology

XRD patterns of IGZO, ZnO and ZnO co-sputtered IGZO films are shown in Figure 2a. The ZnO thin film exhibits strong

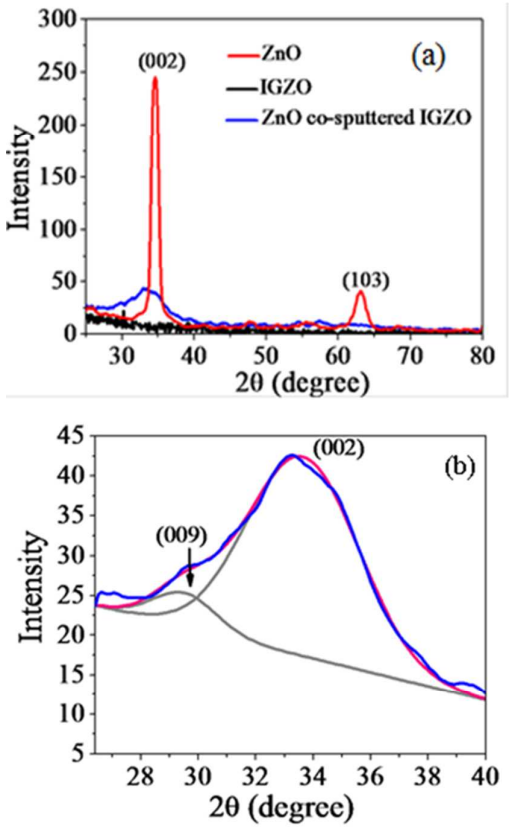

Fig. 2 (a) XRD patterns of IGZO, ZnO and ZnO co-sputtered IGZO films, (b) Gaussian deconvolution curves of the XRD pattern of ZnO co-sputtered IGZO thin film.

reflection along [002] direction with a weak peak corresponds to [103] and displays polycrystalline wurtzite-type hexagonal structure similar to bulk ZnO (JCPDS. File No. 89-0511). The value of average crystallite size (D) as calculated from Scherrer equation ($D = 0.9\lambda/\beta\cos\theta$, λ is the X-ray wavelength, β is the Full width at half maximum value, θ is the Bragg's angle) for ZnO film is ~ 9 nm. In contrast, the IGZO thin film with single target of IGZO is amorphous in nature. The ZnO co-sputtered IGZO film exhibits a broad peak at 2θ~34.55° and seems to be amorphous. The broadening of peak for ZnO co-sputtered IGZO film can be deconvoluted into two broad Gaussian curves centered on [009] and [002] direction (Fig. 2b). It is being caused by the small grain size of ZnO within the amorphous IGZO matrix. Thus, the immiscibility of ZnO and IGZO may lead to formation of amorphous co-sputtered film.

The high resolution transmission electron microscopy (HRTEM) images obtained from the ZnO, IGZO and ZnO co-sputtered IGZO thin films are shown in Fig. 3(a-c). The corresponding fast Fourier transform patterns of the marked HRTEM images are also shown in their inset. Using the spots of the FFT pattern, their inverse fast Fourier transform (IFFT) images are generated (Fig. 3(d-f)). The images are representative of the atomic structure of the materials and growth orientation. The HRTEM image obtained from ZnO film shows that the film is polycrystalline in nature and preferentially oriented along c-axis direction. This is confirmed from the inverse fast Fourier

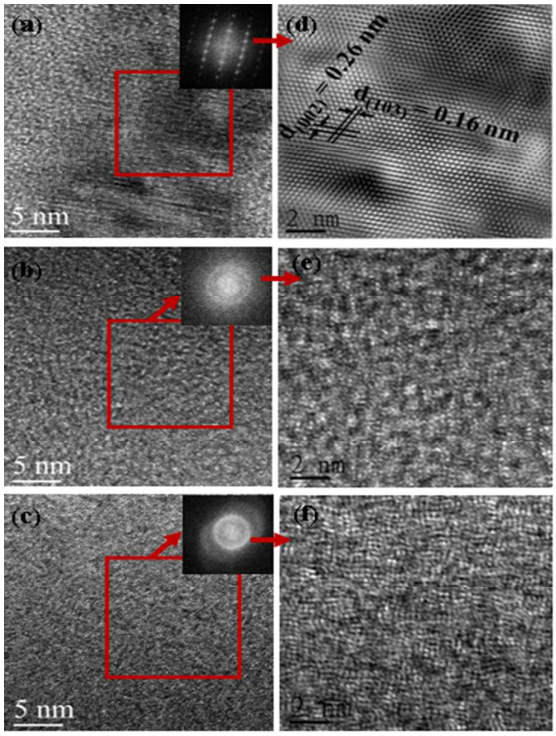

Fig. 3 (a, b, c) -HRTEM images with inset showing FFT patterns of the red marked region; (d, e, f) -Inverse fast Fourier transform images of the corresponding FFT patterns of the ZnO, IGZO and ZnO co-sputtered IGZO thin films, respectively.

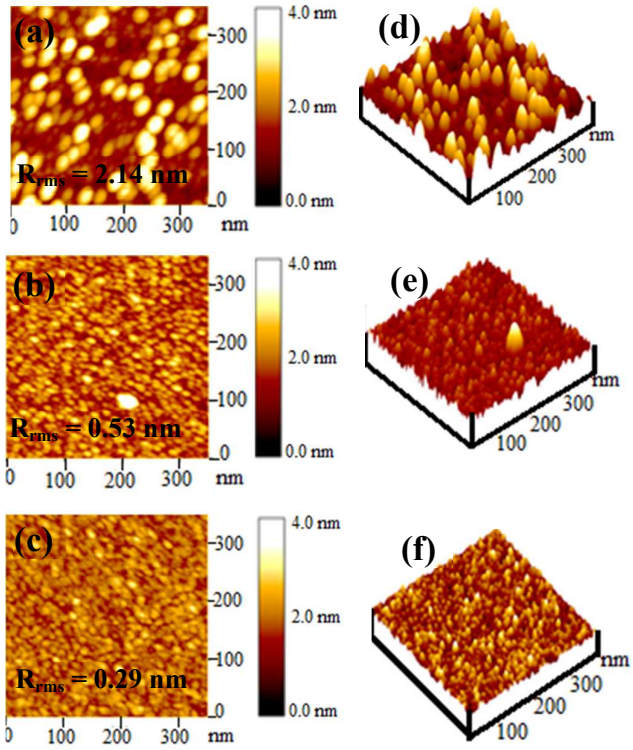

Fig. 4 (a, b, c) -2D and (d, e, f)-3D AFM images of ZnO, IGZO and ZnO co-sputtered IGZO thin films, respectively.

pattern of ZnO (Fig. 3d) which shows lattice planes correspond to particular orientation. The spacing between the two adjacent lattice planes (d) is ~ 2.6 and 1.6 Å correspond to the (002) and (103) plane, respectively and matches well with the value observed from JCPDF file (JCPDS. File No. 89-0511) of bulk ZnO (c ~ 5.2 and a = 3.2 Å). It indicates that dominant crystalline phase is (002) and (103) wurtzite-type hexagonal ZnO and agreed with the XRD observation. The FFT obtained from HRTEM image of IGZO shows circular diffused diffraction pattern (inset of Fig. 3b). It indicates that the IGZO thin film constituted of disorder matrix made of amorphous nanograins (Fig. 3e). In contrast, the ZnO co-sputtered IGZO thin film also appears amorphous as confirmed from the FFT obtained from its HRTEM image (Fig. 3(c, f)). This can be explained as: 1) low temperature deposition provides insufficient energy for surface diffusion and 2) the amorphous phases obviously exhibit lower surface and interfacial energy than those of crystalline counterparts and thus these energies actually favor the formation of an amorphous phase.[13, 14] Consequently, the co-sputtered film exhibits dense and uniform structure without nanopores (Fig. 3(c, f)) .

3.2. Roughness Analysis

Two dimensional (2D) and three dimensional (3D) AFM images of ZnO, IGZO, and co-sputtered films are shown in Fig. 4. The 3-D image (Fig. 4d) of ZnO thin film shows pyramidal shape growth with open voids; the open void and growth both reduces for co-sputtered films. The roughness of the films was analyzed by nanoscope SPM V5 software attached to the AFM instrument by the physical-statistical method. The ZnO thin films show higher roughness value (R_{rms} ~2.1 nm) than the IGZO thin films (R_{rms} ~0.53 nm). It is due to the polycrystalline nature of ZnO thin film which consists of large grains. The ZnO co-sputtered IGZO film is very smooth (R_{rms} ~ 0.29 nm) and featureless without defects such as pinholes, cracks, and protrusion. The uniformity of the ZnO co-sputtered IGZO film was improved due to introduction of Zn (12.22 at.%) in IGZO which causes immiscibility of ZnO within the matrix of In_2O_3.[15] Therefore, the ZnO co-sputtered IGZO thin films showed flat amorphous surface features in order to achieve high performance transparent oxide TFTs.

3.3. XPS Analysis

The surface composition and chemical state have been investigated by XPS, especially for the oxygen contents of the films. The XPS spectra of O1s signal in ZnO thin film can be fitted by three Gaussian distributions, approximately centred at 530.1, 531.5, and 532.6 eV (Fig. 5). The low binding energy (O_L) peak at 530.1 eV is related to O^{2-} ions on the wurtzite-type hexagonal structure which are surrounded by zinc atoms. Therefore, the O_L peak is attributed to Zn-O bonds. The higher binding energy (O_U) peak at 532.6 eV is associated with loosely

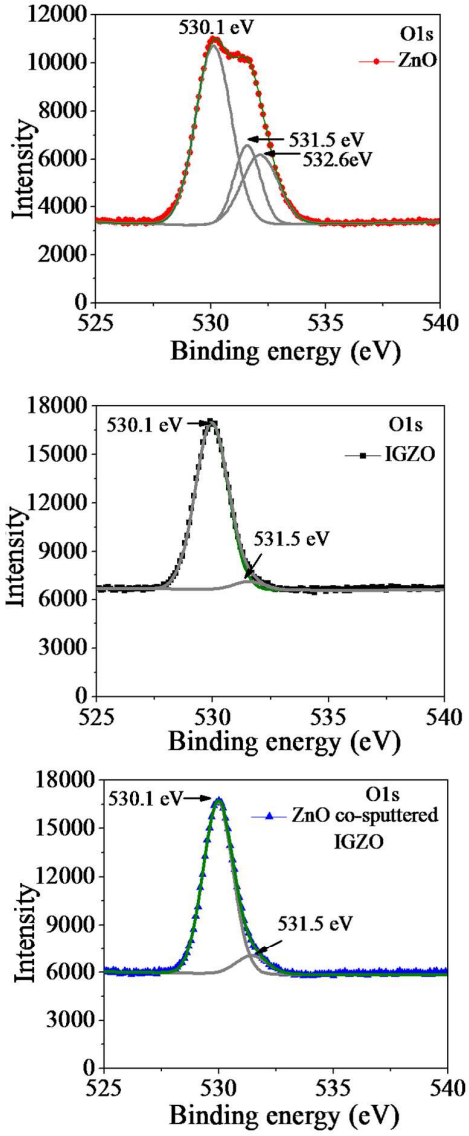

Fig. 5 XPS spectra of O1s for ZnO, IGZO, and ZnO co-sputtered IGZO thin films.

bonded oxygen such as chemisorbed $–CO_3$, adsorbed OH^-, or absorbed H_2O/O_2, on the surface of ZnO thin film. The medium binding energy (O_M) peak at 531.5 eV is attributed to O^{2-} ions that are in oxygen-deficient region within the ZnO matrix.[11] The changes in the intensity of this peak can be connected with the variation in the concentration of the oxygen vacancies. The IGZO and ZnO co-sputtered IGZO film exhibit the binding energy peak of O1s spectra at 530.1 eV and 531.5 eV with disappearance of upper binding energy peak. This indicates that the IGZO and ZnO co-sputtered IGZO films are free from the loosely bonded oxygen as impurities of CO_3, OH^-, H_2O/O_2 on the surface. Notice that, the intensity of medium binding energy peak corresponding to 531.5 eV is higher in the ZnO co-sputtered IGZO than the IGZO films as indicative of higher oxygen vacancies in the ZnO co-sputtered IGZO films. Therefore, the ZnO co-sputtered IGZO film exhibits higher

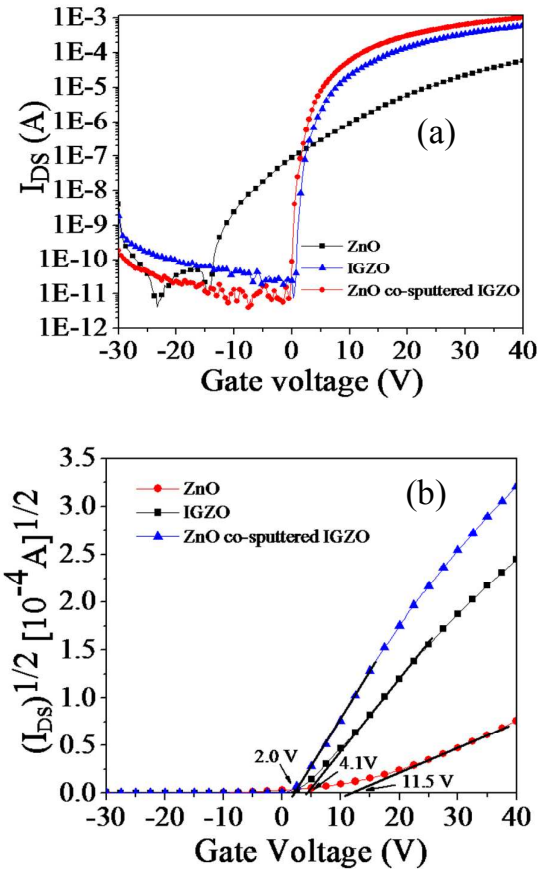

Fig. 6 (a) Semi-log plot of Drain current (I_{DS}) versus Gate voltage (V_{GS}) transfer characteristics for subthreshold swing (SS), (b) $\sqrt{I_{DS}}$ versus V_{GS} plot for threshold voltage (V_{th}) calculation of ZnO, IGZO and ZnO co-sputtered IGZO based TFTs.

carrier concentration (Table 1) and consistent with the Hall measurements.

3.4. Thin film transistors (TFTs)

3.4.1. Electrical characteristics. The transfer characteristics of the TFT devices with ZnO, IGZO and ZnO co-sputtered IGZO thin films as active channel layer are shown in Fig. 6a. The behavior of saturation drain current (I_{DS}) versus V_{GS} at 10 V is different for all the samples. It can be explained by the variation in channel layer compositions. Their electrical performance parameters including threshold voltage (V_{th}), field effect mobility (μ_{FE}), on/off ratio, sub-threshold swing (SS), and interface trap density (N_{it}) are given in Table 1. Notice that, the ZnO TFT exhibits lower mobility and more positive V_{th} (Fig. 6b) than a-IGZO TFT. Interestingly, the TFT with co-sputtered film maintains higher mobility with lower threshold voltage than the a-IGZO TFTs. The lower threshold voltage is ascribed due to high carrier concentration as related to indium doping/oxygen deficiency in the film as observed from the XPS analysis (Fig. 5) and low roughness value (~0.29 nm) (Fig.4c). The high mobility may be attributed to the following reasons

Table 1. Electrical parameters of ZnO, IGZO and ZnO co-sputtered sputtered IGZO based TFTs

TFT Parameters	ZnO	IGZO	ZnO co-sputtered IGZO
μ_{FE} (cm^2/Vs)	2.26	10.50	16.10
V_{th} (V)	11.50	4.10	2.00
S.S (V/decade)	2.17	0.33	0.21
N_{it} (10^{12} $cm^{-3}eV^{-1}$)	7.72	0.99	0.55
I_{on}/I_{off}	8.19×10^4	1.47×10^6	1.04×10^7
I_{DS} (μA) at V_{GS} = 5V	0.40	0.90	3.80
n (10^{17} cm^{-3})	0.45	2.35	4.29

μ_{FE}- Linear field effect mobility, V_{th}-Threshold voltage, SS-Sub-threshold swing voltage, N_{it}- maximum density of surface states, I_{DS}-Saturation drain current, n-Carrier concentration.

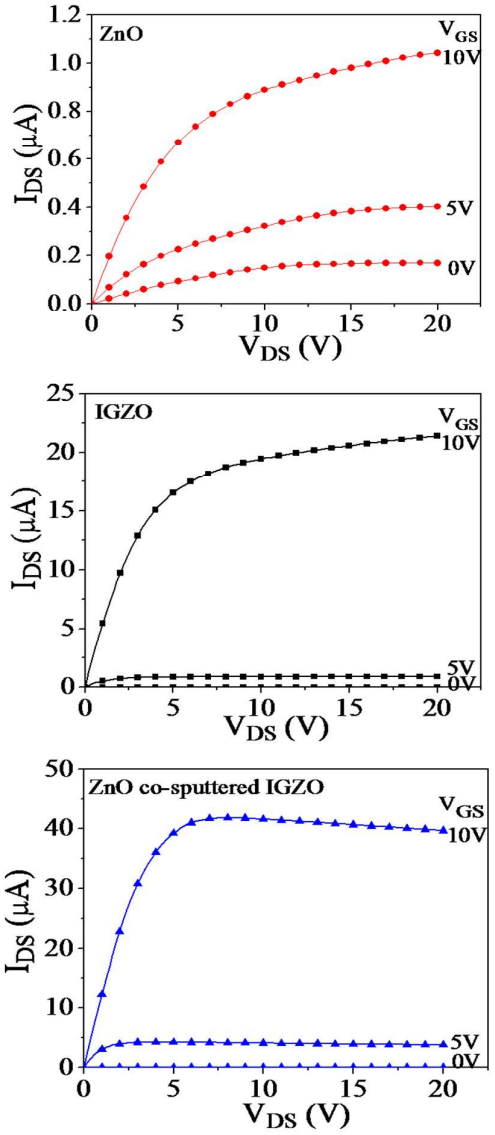

Fig. 7 Output characteristics of the TFTs with ZnO, IGZO, and ZnO co-sputtered IGZO active channel layer.

such as 1) carrier generation from oxygen vacancies as, $V_o \rightarrow (1/2)\ O_2\ (g) + V_O^{++} + 2e$, or extensive overlapping of extended s-orbital of In^{3+} ($[Kr](4d)^{10}(5s)^o$) ion with the neighboring s-orbital of Zn^{2+} ($[Ar](3d)^{10}(4s)^o$) ion to form a conduction path or the both,[16,17] 2) lower roughness value; if the roughness value of the film decreases, that will cause the decrease in the inhabiting of the barriers electron transportation and the mobility will increase. The value of SS (Table 1) for TFTs devices being used to obtain maximum density of surface states, N_{it} = ([{SS $\log_{10}(e)$/ (k_BT/q)}-1](C_i/q), where q is the electronic charge, k_B is Boltzmann's constant, T is absolute temperature, and C_i is the capacitance of gate insulator) is directly related to the roughness and density of the active channel layer.[18,19] The density and molar ratio of zinc cation [Zn/(Zn+In+Ga)] of ZnO, IGZO, and ZnO co-sputtered IGZO films have been measured from the X-ray reflectance (XRR) and Energy-dispersive X-ray (EDX) (Figures are not shown here). The density of films is nearly same (~ 6.68 g/cm^3). However, the molar ratio of zinc cation in ZnO, a-IGZO, and ZnO co-sputtered films is 1, 0.17, and 0.61, respectively and responsible factor to modify the structure and roughness value. This inference indicates that roughness is predominant factor to influence the SS of TFTs. As the R_{rms} roughness value increases, more carriers become trapped and thereby increase in N_{it}. This results in the reduction of SS value for ZnO co-sputtered IGZO films due to low R_{rms} roughness value (Fig. 4c). The flat amorphous surface feature (R_{rms} ~ 0.29 nm) of ZnO co-sputtered IGZO film probably causes smooth contacts between the active channel layer and source/drain electrodes for yielding high I_{on}/I_{off} ratio of 1.04×10^7 [Table 1]. It has been reported elsewhere that a drain current of ~1μA is needed to visible full white gray color in the AMOLED device.[20] In the present work, the saturation drain current (I_{DS}) in the TFTs with ZnO and a-IGZO is 0.4 and 0.9 μA at V_{GS} of 5V, respectively (Fig. 7). The value of saturation drain current gets more improved (I_{DS} ~3.8 μA at V_{GS} = 5 V) (Fig. 7) in the TFT with ZnO co-sputtered IGZO due to its high mobility and low threshold voltage.

3.4.2. Reliability Test of TFTs

In order to analyze the device stability, negative biased illumination stress (NBIS) tests were conducted in dark.

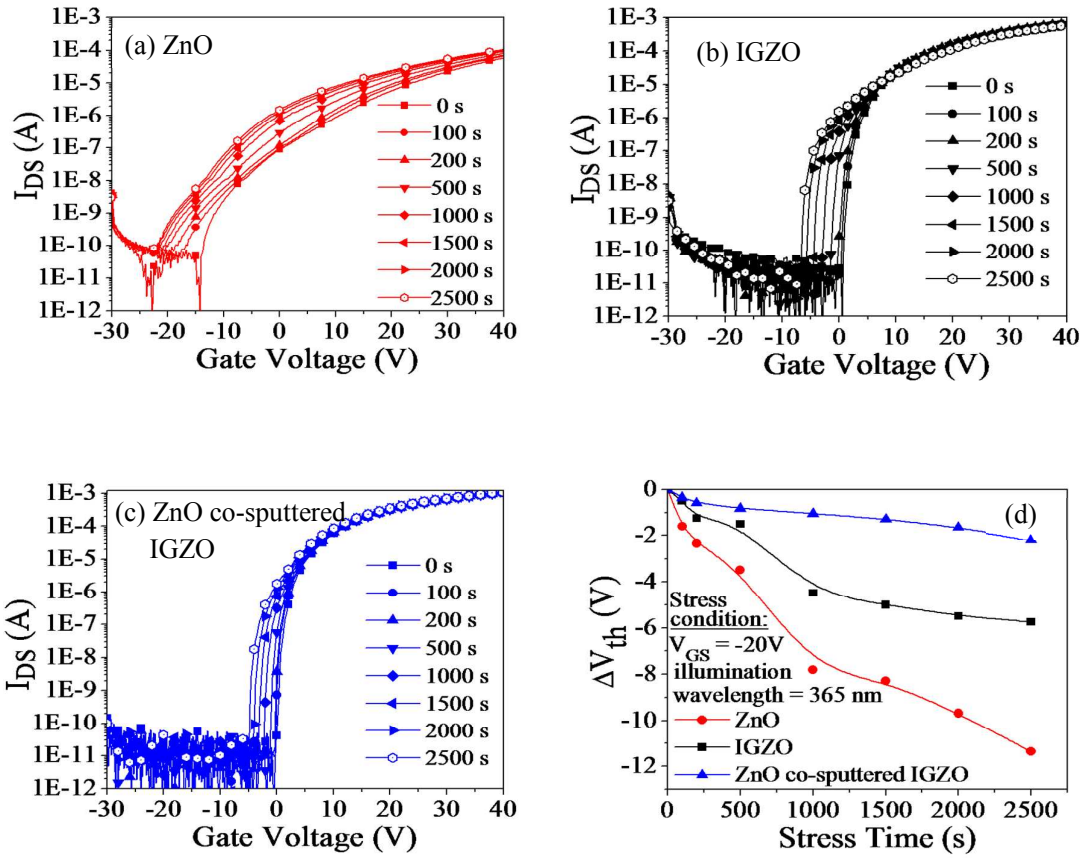

Fig. 8 Transfer characteristics of (a) Single ZnO, (b) Single IGZO, (c) ZnO co-sputtered IGZO TFTs, and (d) ΔV_{th} versus stressing time under NBIS at V_{GS}= -20V with photon energy of 3.39 eV, respectively.

The bias stress was accomplished by biasing the gate at -20V, while the source and drain electrodes were biased at 0V to keep a uniform potential through channel layer. The wave length of light source used for NBIS was 365 nm. The transfer characteristics of the devices before and after illumination for various time periods are shown in Fig. 8 (a-c). The inferior stability of ZnO based TFT was manifested due to large negative threshold voltage shifting under illumination (Fig. 8a). The threshold voltage shifting has been explained by the various proposed concept viz., logarithmic law, photodesorption of oxygen/H_2O, interface modification, grain-boundary trap states, charge trapping and de-trapping stretched-exponential models.[21-25] In this regard, the polycrystalline ZnO exhibits clear grain boundaries with higher roughness value rather than the IGZO and ZnO co-sputtered IGZO thin films-leading thereby to chemisorbed more oxygen as the back channel is exposed to the atmosphere.[26] The adsorbed oxygen species contribute to decrease the carrier density as O_2 + e → $O^-_{2\,(ads)}$. This leads to a positive shift in threshold voltage before the illumination. However, upon illumination, the exposed photons can cause desorption of the O_2^- species which are weakly adsorbed on the back channel surface.[22] The photodesorption of the oxygen species will release free electrons as $O^-_{(ads)}$+ hv → (1/2) O_2 (gas) + $e_{(channel)}$ to the channel layer and cause an increase in net free carrier density. This will result in a more negative shift of threshold voltage in ZnO based TFTs (Fig. 8d). The above mentioned contributions are rather smaller in ZnO co-sputtered IGZO film and would have less negative shift in threshold voltage (Fig. 8d).

4. Conclusions

ZnO, IGZO, and ZnO co-sputtered IGZO thin films have been successfully fabricated for active channel layer in TFTs. This result shows that the polycrystalline nature and pyramidal shape growth of ZnO film leads to higher roughness value. The roughness value decreased for ZnO co-sputtered IGZO films due to immiscibility of ZnO within the matrix of In_2O_3-resulting flat amorphous surface feature for high performance TFT. The low roughness value in ZnO co-sputtered IGZO film results in a low value of SS and threshold voltage shift with high value of Ion/Ioff ratio due to reduced trap density and high smooth drain/source contacts, respectively. In contrast, the high carrier density and low roughness value as well result to high

field effect mobility and high drain current of 3.8 μA at 5V which makes the ZnO co-sputtered IGZO film as a potential candidate for low voltage display applications.

Acknowledgements

This work was supported by Ministry of Science and Technology (MOST) of Taiwan MOST103-2221-E-009-010-MY3 and by Applied Material Corporation.

Notes and references

[a, a*] *Department of Photonics and Display Institute, National Chiao Tung University, Hsinchu, Taiwan, R.O.C., 30010, Fax: +886-3-5737681; Tel: +886-978-628-446; E-mail: nidhi1611@gmail.com, ptliu@mail.nctu.edu.tw,hpshieh@mail.nctu.edu.tw*
[b] *Department of Mechanical Engineering, Vignan University, Guntur-Andhra Pradesh- 522213, India, Tel: +91-8008357245; E-mail: chauhanramnarayan@gmail.com*

1 J. B. Kim, C.F. Hernandez, P. W. J. Jr, X. H. Zhang, and B. Kippelen, *Appl. Phys. Lett*., 2009, **94**, 142107 .
2 S. Z. Bisri, C. Piliego, J. Gao, and M.A. Loi , *Adv. Mater.*, 2014, **26**, 1176.
3 P.T. Liu, Y. T. Chou, L.F. Teng, F. H. Li, and H.P. Shieh, *Appl. Phys. Lett.*, 2011, **98**, 052102.
4 E. Chong, Y. W. Jeon, Y. S. Chun, D.H. Kim and S. Y. Lee, *Thin Solid Films*, 2011, **519**, 4347.
5 P. T. Liu, Y. T. Chou, L.F. Teng, F. H. Li, C. S. Fuh and H.P. Shieh, *IEEE Electron Device Lett.,* 2011, **32**, 1397.
6 N. Tiwari, H. P. D. Shieh and P. T. Liu , *Mater. Lett.*, 2015, **151**, 53.
7 J. C. Park, S. Kim, C. Kim, I. Song, Y. Park, U. I. Jung, D. H. Kim and J.S. Lee, *Adv. Mater.* 2010, **22**, 5512.
8 S. I. Kim, J. S. Park, C. J. Kim, J. C. Park, I. Song and Y. S. Parka, *J. Electrochem. Soc.*, 2009 **156** , H184 .
9 S. Y. Park, B. J. Kim, K. Kim, M. S. Kang, K. H. Lim, T. I. Lee, J.M. Myoung, H. K. Baik, J. H. Cho and Y. S. Kim, *Adv. Mater.* 2012, **24**, 834.
10 D. Afouxenidis, R. Mazzocco, G. Vourlias, P. J. Livesley, A. Krier, W.I. Milne, O. Kolosov and G. Adamopoulos, *ACS Appl. Mater. Interfaces,* 2015, **7**, 7334.
11 R. Zhan, C. Dong, P. T. Liu and H.P.D. Shieh, *Microelectronics Reliability*, 2013, **53**, 1879.
12 C.S. Fuh, P. T. Liu, L.F. Teng, S. W. Huang, Y. J. Lee, H. P. D. Shieh and S. M. Sze, *IEEE Electron Device Lett*., 2013, **34**, 1157.
13 J. J. Yang, Y. Yang, K. Wu and Y. A. Chang, *J. Appl. Phys*., 2005, **98**, 074508.
14 R. Benedictus, A. Bo¨ttger and E. J. Mittemeijer, *Phys. Rev. B*., 1996, **54**, 9109.
15 J.A Lee. J. H. Lee, Y. W. Heo, J. J. Kim and H.Y. Lee, *Curr. Appl. Phys*., 2012, **12**, S89.
16 R. N. Chauhan, R.S. Anand and J. Kumar, *Thin Solid Films*, 2015, **556**, 253.
17 D. Kim, C. Y. Koo, K. song, Y. Jeong and J. Moon, *Appl. Phys. Lett*., 2009, **95**, 103501.
18 J.H. Jeong, H.W. Yang, J.S. Park, J.K. Jeong, Y.G. Mo, H.D. Kim, J. Song and C.S. Hwang, *Electrochem. Solid-State Lett,* 2008, **11**, H157.
19 Y. H. Kim, M. K. Han, J.I. Han, and S. K. Park, *IEEE Trans. Electron Dev,* 2010, **57**, 1009.
20 J.K. Jeong, D.U. Jin, H.S. Shin, H.J. Lee, M. Kim, T.K. Ahn, J. Lee, Y.G. Mo and H.K. Chung, *IEEE Electron Device Lett*., 2007, **28,** 389.
21 A. Suresh and J. F. Muth, *Appl. Phys. Lett*., 2008, **92**, 033502.
22 S. Yang, D.H. Cho, M.K. Ryu, S.H.K. Park, C.S. Hwang, J. Jang and J.K. Jeong, *Appl. Phys. Lett.,* 2010, **96**, 213511.
23 J.M. Lee, I.T. Cho, J.H. Lee and H.I. Kwon, *Appl. Phys. Lett*., 2008 **93**, 093504.
24 Y.G. Chang, T.W. Moon, D.H. Kim, H.S. Lee, J.H. Kim, K.S. Park, C.D. Kim and S. Im, *IEEE Electron Device Lett*., 2011, **32**, 1704.
25 J.J. Siddiquia, J.D. Phillips, K. Leedy and B. Bayraktaroglu, *J. Mater. Res*., 2012, **27**, 2199.
26 R.N. Chauhan, C. Singh, R.S. Anand and J. Kumar, *IEEE Trans. Electron Dev,* 2014, **61**, 3775